MAE 263F Final Report: Snake Project

Sarah Enayati and Jonathan Gray

I. INTRODUCTION

This project aims to design a robotic snake capable of mirroring the movements of biological snakes, enabling it to navigate and operate in challenging environments characterized by a wide range of Reynolds numbers (Re). Such environments are often inaccessible to traditional unmanned aerial vehicles (UAVs), where maneuverability and efficient movement are critical. By leveraging the unique undulatory locomotion patterns of snakes, we aim to develop a versatile robotic platform that can traverse confined spaces, fluid environments, and other complex terrains that challenge conventional robots. Early works by Sir Geoffrey Ingram Taylor explored ways of modeling the motion of long slender animals like snakes and worms swimming through different aqueous environments. Importantly, clear deviations from

To achieve this, we construct an analytical framework that accurately represents snake-like undulation and the associated interactions with viscous fluids. The framework integrates both Resistive Force Theory (RFT) and Slender Body Theory (SBT) to model hydrodynamic forces, providing insights into the behavior of the robotic snake across different fluid regimes. This dual modeling approach allows us to identify the optimal control strategies for movement, taking into account the impact of drag, bending stiffness, and fluid dynamics.

By optimizing the snake's undulatory motion, we aim to achieve more efficient propulsion and better energy management compared to traditional UAVs. This will enable the robotic snake to undertake longer missions with reduced energy expenditure, making it a solution for applications in environments such as underwater inspection, search and rescue, and exploration of confined or hazardous spaces.

II. METHODOLOGY

The goal of this project is to simulate the locomotion of a robotic snake, using a discretized rod model to mimic the motion of a real snake. The snake's movement is modeled by applying both Resistive Force Theory (RFT) and Slender Body Theory (SBT) to understand hydrodynamic interactions in different fluid environments. We created a computational simulation that uses both RFT and SBT to predict the movement of the snake based on various parameters, such as the length of the body, the frequency and amplitude of undulation, and the surrounding fluid's properties.

The snake is modeled as a discretized rod with multiple segments, where each segment represents a portion of the snake's body. The discretization allows the representation of the continuous body as a series of nodes, capturing the bending and undulating movements characteristic of snake locomotion. The number of segments ('nv') can be varied to control the resolution of the model, balancing accuracy and computational cost.

The head motion of the snake is applied by prescribing sinusoidal movements with defined amplitude and frequency. These parameters emulate the undulatory patterns observed in real snakes, generating traveling waves that propagate along the length of the body. The forces and resulting movements of each segment are computed based on the interaction of the snake with the fluid environment.

Two hydrodynamic models are employed to capture the interaction of the snake with the surrounding fluid. Resistive Force Theory (RFT) is used to calculate drag forces that act on each segment of the snake, assuming that each segment independently interacts with the fluid, with drag coefficients (C_t and C_n) characterizing the tangential and normal resistance, respectively. This approach provides a simplified model to approximate the local effects of drag along the body.

Slender Body Theory (SBT) is implemented to incorporate more complex hydrodynamic interactions between different segments of the snake's body. Unlike RFT, SBT accounts for the long-range influence of one segment on others by considering hydrodynamic interactions along the length of the snake. The SBT approach uses a discretized version of the Stokeslet interaction kernel to compute these forces.

The governing equations of motion for the snake are solved iteratively using a Newton-Raphson method. Forces due to bending, stretching, and hydrodynamic drag are combined to compute the net force acting on each segment. The bending and stretching energies are modeled based on the material properties of the rod, such as Young's modulus ('Y'), which controls the stiffness of the snake. The iterative solver is used to update the positions of each segment at each time step, taking into account hydrodynamic forces calculated via RFT or SBT.

We use Reynolds number to verify the validity of the SBT and RFT models in different regimes. Specifically, SBT is most accurate when the Reynolds number is low, as it assumes that inertial effects are negligible compared to viscous forces. Therefore, if the Reynolds number is found to be high and the results from SBT and RFT match closely, this suggests an inconsistency in the physical assumptions of SBT. In our project, we use the Reynolds number as a key indicator to ensure that each hydrodynamic model is used appropriately. If discrepancies arise between the predicted results from RFT and SBT at high Reynolds numbers, it indicates that the SBT model is being applied outside its valid range, and these results are examined to better understand the conditions under which each model is appropriate.

To understand the effect of various parameters on the

snake's locomotion and determine optimal parameters, sensitivity analyses were performed by varying key parameters, specifically, the number of nodes and the length of the snake. These analyses help identify optimal conditions for efficient movement and quantify how different factors contribute to the dynamics of the snake. In particular, sensitivity analysis was conducted to optimize the x-velocity of the head by varying the length of the rod and the number of segments. This allowed us to determine the ideal configuration for maximizing forward propulsion, taking into account both fluid interactions and the physical properties of the snake.

A. Stability Considerations for Slender Body Theory

The SBT method is highly sensitive to both temporal and spatial discretization parameters. During our simulations, we found that achieving numerical stability with SBT required careful tuning of both the time step and the number of nodes (discretized segments of the snake's body).

Initially, we observed that SBT was prone to numerical instability, particularly for higher node counts and larger time steps. These instabilities manifested as rapidly diverging errors in the Newton solver, as well as non-physical behaviors such as unrealistic forces and velocities. To mitigate these issues, we experimented with the discretization parameters. We ultimately determined that maintaining a small time step of 0.003 and reducing the number of nodes to 3 provided a stable simulation environment for SBT.

III. Sensitivity Analysis for Parameter Determination

In our sensitivity analysis, we use the average x-direction velocity as our performance metric to evaluate the effects of different parameters (number of nodes, length of snake, and hydrodynamic influence range) on the locomotion efficiency of the robotic snake. The x-direction velocity represents the snake's forward speed, which indicates how well it can propel itself through a fluid environment using undulation.

A. Nodal Determination

We vary the number of nodes in the robotic snake to understand its effect on locomotion efficiency and average velocity and thus determine the optimal number of nodes for our snake. The number of nodes determines how well the wave propagates along the body, directly impacting the smoothness of movement and overall propulsion. As we increase the number of nodes from 5 to 25, we observe a significant improvement in average velocity [see Figure 1.] A higher number of nodes allows for smoother and more continuous undulatory movement, which generates more effective thrust. However, beyond 11 nodes, the velocity begins to plateau, with only minimal increases up to 13 nodes. This plateau suggests that additional nodes do not significantly enhance propulsion but instead add computational complexity and potentially increase drag resistance. Based on these results, we choose the optimal number of nodes to be 12. This balances achieving high velocity and minimizing unnecessary computational load,

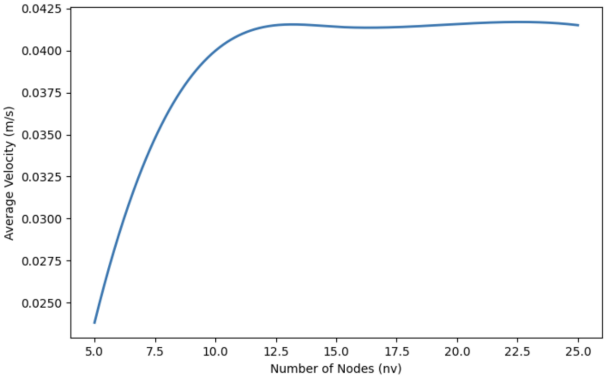

Fig. 1. Sensitivity Analysis on Number of Nodes

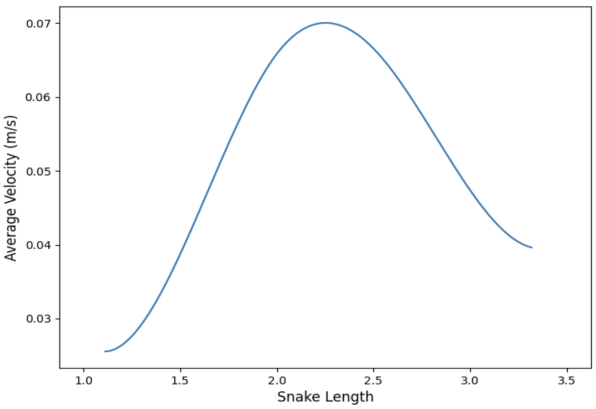

Fig. 2. Sensitivity Analysis on Snake Length

and ensures efficient movement without overcomplicating the model or reducing performance due to added drag.

B. Snake Length

We also conducted sensitivity analysis on the total length of the robotic snake to understand its influence on locomotion efficiency and average velocity. The length of the snake is a critical parameter because it affects both the wave propagation dynamics and the drag experienced by the body as it moves through the fluid. A longer snake generally allows for more undulation cycles along its body, which can generate greater propulsion due to more efficient transmission of waves. However, this increased length also results in more surface area interacting with the fluid, therefore increasing drag resistance. The longer the snake, the greater the cumulative drag that each segment must overcome, which can result in decreased average velocity. On the other hand, a shorter snake experiences less overall drag, which may increase velocity, but it may also lack the sufficient wave propagation length needed to generate effective thrust. This would lead to reduced propulsion efficiency. By analyzing different snake lengths, we evaluated the trade-off between propulsion generation and fluid resistance, which allowed us to identify an optimal length that maximizes velocity while maintaining stability.

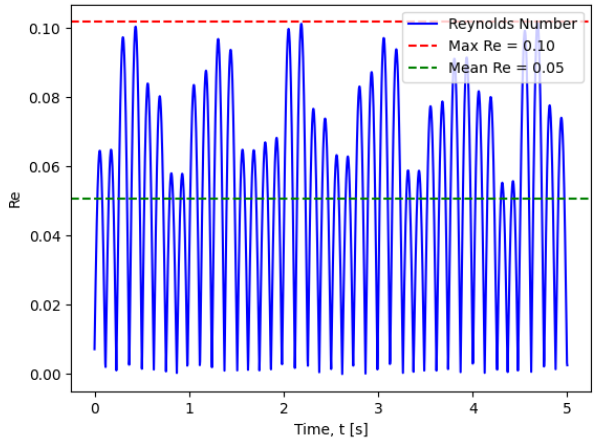

Fig. 3. Reynolds Number

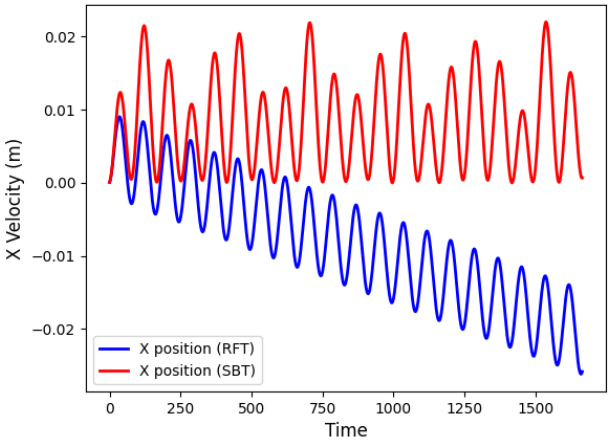

Fig. 5. X-position or SBT and RFT

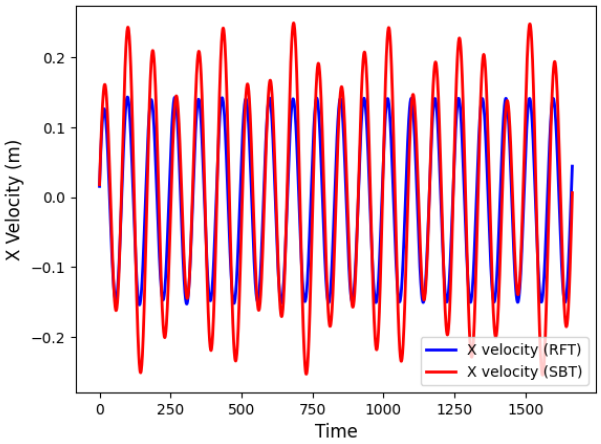

Fig. 4. X-velocity or SBT and RFT

In our sensitivity analysis of the robotic snake's total length, we vary the rod length from 1.0 to 2.0 meters and observe its effect on the average velocity, as can be seen in Figure 2.

These results indicate that as the snake length increases, the average velocity initially improves, but starts declining again after reaching a peak of 2.2 meters. This is due to the increase in drag resistance as the length increases further, ultimately reaching a point where the additional surface area interacting with the fluid negates the propulsion gains. Based on these results, a snake length of 2.2 meters is optimal, as it maximizes average velocity without introducing significant drag penalties.

IV. Validation for SBT/RFT Methods

A. Reynolds Number Analysis

In this project, the Reynolds number (Re) was used to verify the validity of the RFT and SBT methods for modeling the motion of our snake. The Reynolds number represents the ratio of inertial forces to viscous forces, and for SBT, the assumptions hold true only under conditions of very low Reynolds numbers ($R << 1$), where viscous forces dominate. We chose the viscosity to be sufficiently high to keep the Reynolds number much less than 1. This allowed us to ensure that both theories could be reasonably compared under conditions where they are valid, and that the assumptions behind SBT were not violated.

The comparison between RFT and SBT, seen in figures 4 and 5, revealed several insights. With the low Reynolds number, both methods produced results that were closely aligned, particularly in terms of the velocity of the snake. The plots demonstrated that at these conditions, the SBT and RFT predictions for x-velocity and x-position tracked similarly, with minor deviations that may be attributed to the inherent simplifications and assumptions in each theoretical approach. Importantly, the use of high viscosity ensured that the Re values remained consistently low, validating the applicability of both models in this scenario.

B. Viscosity Effects on Velocity (RFT)

We model viscosity versus velocity to validate our RFT model. The results demonstrate a clear relationship between the fluid viscosity (μ) and the average velocity of the snake's motion. Three cases were analyzed with viscosities of μ = 1.1, 1.9, and 3.0, respectively. As viscosity increases, the absolute value of the average velocity decreases, reflecting the increased resistance of the fluid to the snake's motion. For μ = 1.1, the average velocity is -0.0513 m/s, while for μ = 1.9 and μ = 3.0, the average velocities are -0.0497 m/s and -0.0425 m/s, respectively. This aligns with theoretical expectations, as higher viscosity corresponds to greater drag forces acting on the snake.

The oscillatory behavior in the velocity profiles is also influenced by the fluid's viscosity. In lower-viscosity fluids, the velocity amplitudes are larger due to reduced resistance, allowing the snake to generate greater propulsion during its undulatory cycles. Conversely, higher viscosity dampens these

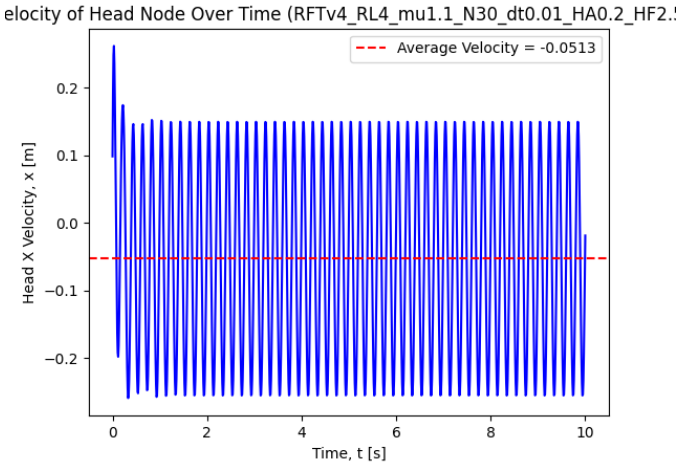

Fig. 6. Viscosity Effects on Velocity at $\mu = 1.1$

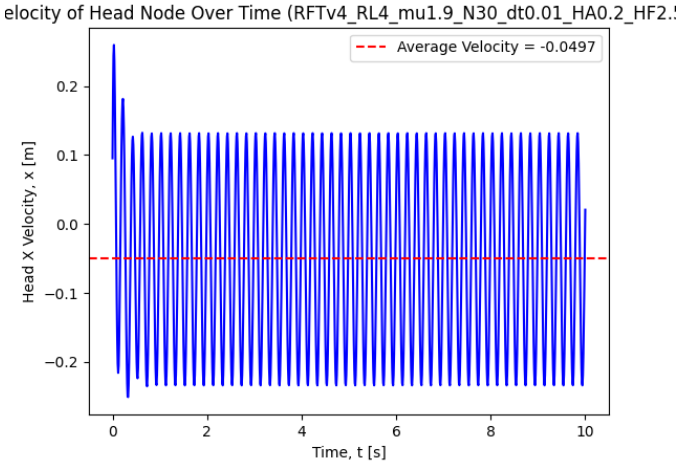

Fig. 7. Viscosity Effects on Velocity at $\mu = 1.9$

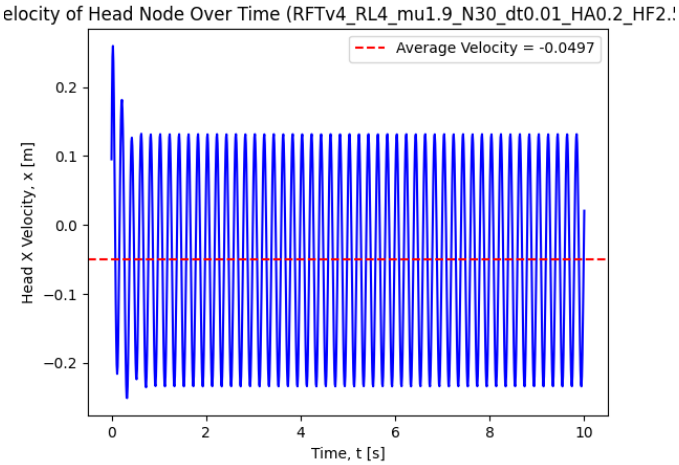

Fig. 8. Viscosity Effects on Velocity at $\mu = 3$

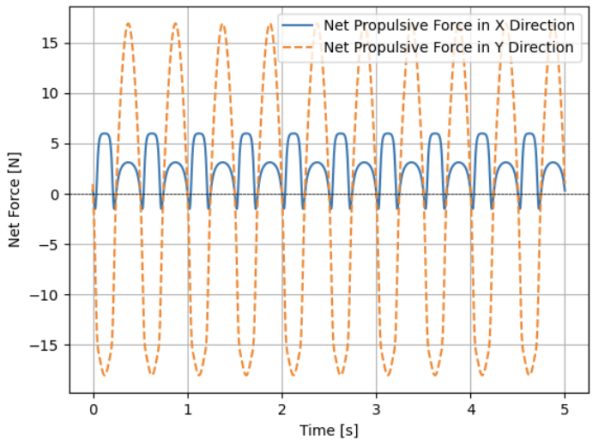

Fig. 9. Net Propulsive Forces (RFT)

oscillations, resulting in smaller amplitude variations. Despite these differences, the negative average velocity across all cases confirms consistent directional movement.

C. Net Propulsive Force Validation (RFT)

We analyze of the net propulsive forces to validate our RFT model. According to RFT, the motion of the snake generates different forces depending on the direction of movement relative to the surrounding medium. This should result in a net forward force in the x-direction, while the forces in the y-direction should oscillate back and forth around zero without contributing to any net motion.

The plot of net propulsive forces matches these expectations. In the x-direction, the force oscillates over time but has a positive average, indicating that the snake is consistently moving forward. This positive average force confirms that the forward propulsion created by the snake's undulating motion is correct. In the y-direction, the forces show a clear pattern of oscillation that averages to zero, which is expected since the side-to-side motion of the snake cancels out over each full movement cycle.

The periodic nature of the forces in both directions further supports the accuracy of the model. The oscillations in the x-direction reflect the natural variation in forward thrust as the snake moves through its cycle of motion, while the y-direction oscillations capture the back-and-forth forces caused by the body's side-to-side motion. The absence of any unusual trends or imbalances in the forces suggests that the model is accurately capturing the mechanics of the snake's movement.

D. Mechanical Power (RFT)

The plot of mechanical power over time serves as another important validation for the RFT model. The mechanical power reflects the work done by the snake to propel itself through its undulating motion. For the RFT model to be valid, the power should oscillate in a periodic manner, as the snake's

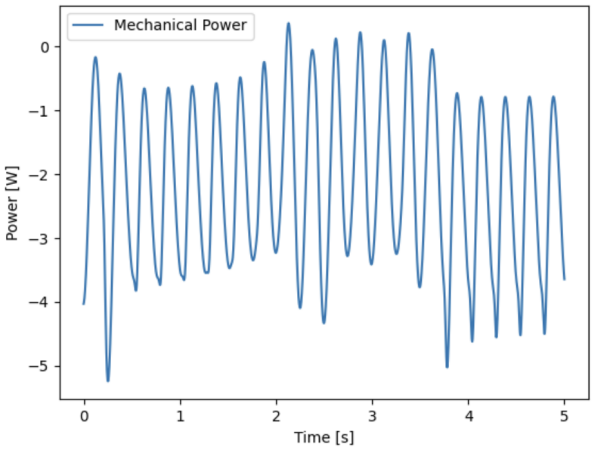

Fig. 10. Mechanical Power over Time (RFT)

motion involves cycles of propulsion and resistance due to the surrounding medium.

This plot exhibits the expected periodic behavior, with power oscillating between peaks and troughs. The negative values indicate that the snake is consistently expending energy to overcome drag forces, which is typical for locomotion in a resistive medium. The amplitude of the oscillations suggests that the energy expenditure varies throughout the motion cycle, with certain phases requiring more work to maintain propulsion.

The stability of the oscillations over time confirm that the model is functioning as intended. There are no irregular spikes or disruptions in the power, which would indicate numerical or modeling errors. Additionally, the gradual increase in amplitude during the initial phase of motion aligns with the expectation that the snake needs to build momentum before reaching a steady-state movement.

V. Appendix A

Algorithm 1 Get Hydrodynamic Force (getFh)

Input: $q_{new}, q_{old}, C_t, C_n, range, nv$
Output: F_{hydro}, J_{hydro}
for each node, k, in snake body: do
  // tangents and normals are calculated
  $\hat{t} = \frac{q_{k+1}-q_k}{|q_{k+1}-q_k|}$
  $\hat{n} = [-\hat{t}[1], \hat{t}[0]]$
  // tangential and normal velocity and forces are calculated
  $v_t = u_k \cdot \hat{t}$
  $v_n = u_k \cdot \hat{n}$
  $F_t = -C_t * v_t$
  $F_n = -C_n * v_n$
  // Hydrodynamic force is updated for all DOF
  $F_{hydro} = F_{hydro} + F_t + F_n$
  // Hydrodynamic Jacobian is updated for all DOF
  $J_t = \frac{-C_t}{dt} * \hat{t} \otimes \hat{t}$
  $J_n = \frac{-C_n}{dt} * \hat{n} \otimes \hat{n}$
  $J_{hydro}[k,k] = J_{hydro} + J_t + J_n$
  for each node, j, in range: do
    $J_{stokeslet} = \frac{(I+\hat{r}\otimes\hat{r})}{8\pi\mu|r|}$
    $F_{interaction} = J^{-1}_{stokeslet} v_{rel}$
    $F_{hydro}[k] = F_{hydro}[k] + F_{interaction}$
    $F_{hydro}[j] = F_{hydro}[j] - F_{interaction}$
    $J_{interaction} = \frac{-J_{stokeslet}\Delta L}{|r|}$
    // Update Jacobian
    $J_{hydro}[k,j] = J_{hydro}[k,j] + J_{interaction}$
    $J_{hydro}[j,k] = J_{hydro}[j,k] - J_{interaction}$
  end for
end for
Return F_{hydro}, J_{hydro}

Algorithm 2 Snake Locomotion Simulation

Input: tol
Output: ...
$err \leftarrow \infty$
while $err > tol$ **do**
  // Stretching and bending forces calculated from predefined functions
  // Calculate viscous force and its Jacobian (using RFT)
  // Calculate hydrodynamic force and hydrodynamic interaction forces (getFh)
  $F_{hydro} = getFh(q_{new}, q_{old}, C_t, C_n, nv)$
  // Calculate Equation of Motion
  $f = M * \frac{q_{new}-q_{old}}{\Delta t^2} - M * \frac{u_{old}}{\Delta t^2} - (F_b + F_s + F_{hydro})$
end while

References

[1] A. Yamano, K. Shimizu, M. Chiba, H. Ijima, Fluid force identification acting on snake-like robots swimming in viscous fluids, Journal of Fluids and Structures, Volume 106, 2021, 103351, ISSN 0889-9746, https://doi.org/10.1016/j.jfluidstructs.2021.103351

[2] A. Yamano, T. Kimoto, Y. Inoue, M. Chiba, Optimal swimming locomotion of snake-like robot in viscous fluids, Journal of Fluids and Structures, Volume 123, 2023, 104007, ISSN 0889-9746, https://doi.org/10.1016/j.jfluidstructs.2023.104007.

[3] Moore, B. R. (n.d.). Snake locomotion. University of Louisiana at Lafayette. Retrieved October 30, 2024, from https://userweb.ucs.louisiana.edu/brm2286/locomotn.htm

[4] Cicconofri, G., & DeSimone, A. (2015). A study of snake-like locomotion through the analysis of a flexible robot model. *Proceedings of the Royal Society A: Mathematical, Physical and Engineering Sciences, 471*(2182), 20150054. https://doi.org/10.1098/rspa.2015.0054

[5] Kimoto, T., Yamano, A., & Chiba, M. (2023). Estimation of fluid forces on a snake-like robot swimming in viscous fluids considering boundary layer thinning. In *2023 IEEE/SICE International Symposium on System Integration (SII)* (pp. 1-6). IEEE. https://doi.org/10.1109/SII55687.2023.10039336

[6] G. Taylor, "Analysis of the Swimming of Long and Narrow Animals," *Proceedings of the Royal Society of London. Series A, Mathematical and Physical Sciences*, vol. 214, no. 1117, pp. 158-183, Feb. 1952.
[7] Païdoussis, Michael P., Stuart J. Price, and Emmanuel De Langre. Fluid-structure interactions: cross-flow-induced instabilities. Cambridge University Press, 2010
[8] Jawed, M. Khalid, Alyssa Novelia, and Oliver M. O'Reilly. *A primer on the kinematics of discrete elastic rods*. Berlin/Heidelberg, Germany: Springer International Publishing, 2018.
[9] Gray, James. "The mechanism of locomotion in snakes." Journal of experimental biology 23.2 (1946): 101-120.
[10] Rodenborn, Bruce, et al. "Propulsion of microorganisms by a helical flagellum." *Proceedings of the National Academy of Sciences* 110.5 (2013): E338-E347